Title;

Functional expression of M3, a muscarinic acetylcholine receptor subtype, in taste bud cells of mouse fungiform papillae.

Authors;

Kohgaku Eguchi, Yoshitaka Ohtubo and Kiyonori Yoshii.

Affiliation;

Graduate School of Life Science and Systems Engineering, Kyushu Institute of Technology.

Running head;

Expression of M3 in fungiform taste bud cells

Contact Information;

Kiyonori Yoshii. Kyushu Institute of Technology, Hibikino 2-4, Graduate School of Life Science and Systems Engineering, Kyushu Institute of Technology, Kitakyushu 808-0196, Japan, yoshii@brain.kyutech.ac.jp

Abstract

Taste bud cells (TBCs) express various neurotransmitter receptors assumed to facilitate or modify taste information processing within taste buds. We investigated the functional expression of muscarinic acetylcholine receptor (mAChR) subtypes, M1-M5, in mouse fungiform TBCs. ACh applied to the basolateral membrane of TBCs elevates the intracellular Ca^{2+} level in a concentration-dependent manner with the EC_{50} of 0.6 μM. The Ca^{2+} responses occur in the absence of extracellular Ca^{2+}, and are inhibited by atropine, a selective antagonist against mAChRs. The order of IC_{50}s examined with a series of antagonists selective to mAChR subtypes show the expression of M3 on TBCs. Perforated whole-cell voltage-clamp studies show that 1 μM ACh blocks an outwardly rectifying current, and that 100 nM atropine reverses the block. RT-PCR studies suggest the expression of M3, but not the other mAChR subtypes. Immunohistochemical studies show that PLCβ2-immunoreactive TBCs and SNAP-25-immunoreactive nerve endings are immunoreactive to a transporter that packs ACh molecules into synaptic vesicles (VAChT). These results show that M3 occurs on a few fungiform TBCs, and suggest that a few nerve endings, and probably a few TBCs, release ACh by exocytosis. The role of ACh in taste responses is discussed.

Key words; immunohistochemistry, whole-cell-clamp, Ca^{2+}-imaging, pharmacology, RT-PCR, vesicular acetylcholine transporter.

Introduction

Acetylcholine is a measure neurotransmitter received by two main classes of receptors, the muscarinic ACh receptors (mAChRs) and the nicotinic ones. In the autonomic nervous system, postganglionic parasympathetic neurons release ACh, as postganglionic sympathetic neurons release noradrenaline. The involvement of ACh has been suggested in peripheral taste responses, typically in mammals. Physiological studies showed that the intravenous injection of ACh enhanced rat taste nerve responses (Kimura 1961), and that the block of its degradation selectively enhanced the amplitude of the neural responses to sour and salty stimulation in rats (Sakai 1965), though neither the block of ACh degradation nor the application of nicotinic ACh receptor agonists enhanced frog taste nerve responses (Duncan 1964). Also biochemical studies showed that ACh esterase concentration was high in rat taste buds (Paran *et al.* 1975), and that carbachol, an ACh agonist, enhanced inositol turnover in rat lingual tissue (Hwang *et al.* 1990). Recent studies with Ca^{2+} imaging and immunohistochemical techniques showed the expression of M1, a subtype of five mAChR subtypes M1-M5, on rat and mouse taste bud cells (TBCs)(Ogura 2002; Ogura *et al.* 2005). However, the expression of the other mAChR subtypes in TBCs remained to be investigated.

In this study, we investigated the expression of five mAChR subtypes in mouse fungiform TBCs and, for comparison, in mouse circumvallate papillae that contained lingual epithelial cells in addition to TBCs with a variety of techniques including reverse transcriptase-mediated polymerase chain reactions (RT-PCR), Ca^{2+}-imaging, and perforated whole-cell voltage-clamping. Also the expression of a transporter that packs ACh molecules into synaptic vesicles (VAChT) was investigated, though the expression of VAChT somewhere in mouse taste tissue was reported in an abstract form without figures (Ogura *et al.* 2005). Here we show that TBCs express M3 and VAChT, and nerve endings express VAChT in fungiform papillae. Also, we show the expression of VAChT in circumvallate TBCs and suggest the expression of M1, M3, M4, and M5 in circumvallate papillae. The role of ACh in taste responses is discussed.

Materials and Methods

Peeled lingual epithelia

We prepared peeled lingual epithelia containing taste buds in fungiform papillae as described previously (Furue *et al.* 1997), in accordance with Guiding Principles for the Care and Use of Animals in the Field of Physiological Sciences approved by the Council of the Physiological Society of Japan. In brief, we sacrificed mice by decapitation after the anaesthetization with ether, removed tongues, and subcutaneously injected them with an elastase solution (the composition of this and other solutions are summarized in "Solutions", unless otherwise noted). After 10~12-min incubation in Earle's solutions bubbled with 95% O_2 / 5% CO_2 at 25 °C, we exposed the basolateral membranes of TBCs by peeling the lingual epithelium with forceps, mounted the peeled epithelium on a recording platform with the basolateral membrane side upward, and placed the platform under a 60x-water-immersion objective (Fluor-60X, Olympus, Tokyo, Japan, Fig.1A). The basolateral membrane side of peeled epithelia was irrigated with either a physiological saline or test solutions by exchanging the composition of the water-column between the water-immersion objective and the basolateral membrane side. The receptor membrane side facing inside the platform was acclimated to the physiological saline, unless otherwise noted. Peeled lingual epithelia containing circumvallate papillae and those containing no taste buds (non-taste lingual epithelia) were similarly prepared for RT-PCR and immunohistochemical studies.

Ca^{2+}-imaging

After mounted the peeled epithelium on the recording platform, we soaked the basolateral membrane side of the peeled epithelium in a fura-2 AM solution for 30 min at 37 °C, washed with the physiological saline, and then placed under a fluorescent microscope equipped with the water-immersion objective. ACh and other test substances were dissolved in the physiological solution or in a Ca^{2+}-free solution, and applied to the basolateral membranes of TBCs (Fig.1*A*).

Fura-2-stained TBCs were excited at 340 and 380 nm with a spectroscope type high-speed wavelength changer (C7773, Hamamatsu Photonics, Hamamatsu, Japan). Images of fura-2 fluorescence were acquired every 2.5 s with an intensified CCD camera through the water-immersion objective, stored in a computer, and analyzed with AQUACOSMOS software (version 2.0, Hamamatsu Photonics). Averaged intracellular Ca^{2+} levels, $[Ca^{2+}]_{in}$, over respective cell areas were sequentially plotted as

a ratio of F340/F380. Responses to test solutions were defined as deflections above the mean resting $[Ca^{2+}]_{in}$ (obtained by averaging 5 data points during the pre-test control period). The response magnitude was calculated as the peak deflection magnitude normalized to the deflection magnitude for 10 μM Ach, and plotted data were mean ± SD of these normalized responses, unless otherwise noted.

Isolation of taste buds and purification of taste bud RNA

Lingual epithelia containing fungiform TBCs were peeled as mentioned above except that we injected tongues with an enzyme solution consisted of 0.1 % elastase and 0.2 % protease dissolved in the physiological saline, and that we incubated them in the physiological saline for 4 min at 25 °C. Each peeled epithelium was mounted with the basolateral membrane side upward on the recording platform, and was treated with an EGTA solution for 1 min to loosen the connections between taste buds and perigemmal cells, their surrounding tissues. The loosened taste buds were picked up from the peeled epithelia with a micropipette. We collected 30 taste buds for each RT-PCR and extracted total RNA with ISOGEN (Nippon Gene, Tokyo, Japan); we harvested a single taste bud a time and immediately placed it in ISOGEN. Extracted total RNA was incubated with DNase I (Takara Bio, Otsu, Japan) and RNase inhibitor (Takara Bio), in a 20 μl final volume, to remove any contaminating genomic DNA.

Similarly, we prepared mouse lingual epithelia containing circumvallate papillae, extracted total RNA from the epithelia, and incubated extracted RNA. Note that circumvallate taste buds were not isolated. For positive and negative controls, RNA was extracted from brain tissue and lingual epithelia containing no taste buds.

RT-PCR

The cDNA synthesis and PCR were carried out using OneStep RT-PCR Kit (QIAGEN, Valencia, CA). After isolation of RNA, 1 μl of total RNA was added to a RT-PCR mix containing 0.6 μM forward and reverse primers (Table 1). Conditions for RT-PCR were; reverse transcription, 55 °C for 30 min; initial PCR activation step, 94 °C for 7.5 min; denaturation, 40 cycles at 94 °C for 30 sec; annealing, 54-62 °C for 1 min; extension, 72 °C for 3 min; final extension, 72 °C for 10 min. Annealing temperatures were; 54 °C for M5 and α-gustducin; 58 °C for M1-M4 and β-actin; 62 °C for VAChT. Optimum annealing temperatures were obtained by preliminary PCR experiments on brain mRNA; we tested a range of annealing temperatures from 50 °C to 62 °C in 4 °C steps, and took an annealing temperature that yielded a clear single band with a correct size on agarose gels for each primer set. PCR products were analyzed by 2 % agarose gel electrophoresis, stained with ethidium bromide (0.1 μg/ml), and visualized by UV

illumination. PCR products and primers were submitted to Genenet (Fukuoka, Japan), where the identity of the band of interest (PCR product of expected size) was confirmed by sequencing.

Perforated whole-cell voltage-clamping

Whole-cell-clamp conditions were similar to our previous papers (Higure *et al.* 2003; Ohtubo *et al.* 2001) except the use of amphotericin B for perforated whole-cell clamping. In brief, electrical responses were recorded with glass electrodes (4~7 MΩ) filled with an amphotericin B electrode solution, amplified with an voltage-clamp amplifier (Axopatch 200B, Molecular Devices, Sunnyvale, CA, USA), filtered at 10 kHz, digitized with an A/D converter (Digidata 1200, Axon Instruments), and stored using pCLAMP data acquisition and analysis software (ver. 8.2, Axon Instruments) on a personal computer. The liquid junction potential of ~ 5 mV between recording and reference electrodes was neglected.

Immunohistochemistry

We immunohistochemically investigated fungiform TBCs in the peeled epithelia without slicing after the fixation and immunohistostaining described as follows. The peel lingual epithelia containing fungiform TBCs were treated with Zamboni solution at 4 °C overnight. After a brief wash in PBS, the epithelia were incubated in a citric acid buffer for 20 min at 85 °C. After six 10-min washes with PBS, the epithelia were incubated in a blocking solution containing 3% normal donkey serum, 0.3% Triton X, and 1% bovine serum albumin in PBS for 4 h.

Circumvallate TBCs were transcardially fixed by the perfusion with PBS followed by Zamboni solution. The tongue was then postfixed with Zamboni solution for 2 h before incubated with PBS containing 30 % sucrose overnight. Circumvallate papilla were embedded in OCT compound (Tissue-Teck, Sakura Finetek Japan, Tokyo, Japan), frozen, and cut with a cryostat into 10-μm-thick sections, and immunohistostained.

We incubated the epithelia and sections with primary antibodies (Table 2) dissolved in the blocking solution at 4 °C for 48 h, rinsed with PBS, and incubated with the Alexa fluor-conjugated secondary antibodies (Table 2) dissolved in the blocking solution at 4 °C overnight. The epithelia were washed with PBS, and then mounted on glass slides with 50% glycerol and 0.1 mg/ml p-phenylenediamine (PPDA) dissolved in PBS. Fluorescence images of fungiform TBCs in the horizontal, optical slices of whole-mount preparations and those of circumvallate TBCs in 10-μm-thick sections were obtained with a laser scanning confocal microscope system (Leica Microsystems,

Bensheim, Germany).

For control purposes, the primary antibody against VAChT was preadsorbed with a 10-fold molar excess of the synthetic antigen to the normal antibody dilution for 2 h at 37 °C. After the antigen-antibody mixture was spun at 15,000 g for 30 minutes, the supernatant was used for the primary antibody in the usual immunohistochemical protocol.

Solutions

Unless stated otherwise, all reagents for physiological experiments were obtained from Wako (Osaka, Japan). All solutions were prepared with deionized water and the components were expressed in millimolar concentrations, unless otherwise noted. Physiological saline; 150 NaCl, 5 KCl, 2 $CaCl_2$, 0.5 $MgCl_2$, 10 glucose, and 5 HEPES (Sigma, St. Louis, MO), buffered to pH 7.4 with NaOH. Amphotericin B electrode solution; 130 KCl, 15 NaCl, 5 HEPES, 166 μg/ml Amphotericin B, 250 μg/ml Pluronic F-127 (Sigma), buffered to pH 7.2 with KOH. Citric acid buffer; 1.8 citric acid monohydrate, 8.2 trisodium citrate dehydrate, buffered to pH 7.0 with NaOH. The Ca^{2+}-free solution was prepared by replacing $CaCl_2$ with $MgCl_2$ in the physiological saline. Earle's solution; 116 NaCl, 5.4 KCl, 1.8 $CaCl_2$, 0.8 $MgSO_4$, 26.2 $NaHCO_3$ and 1 NaH_2PO_4. EGTA solution; 137 NaCl, 2 EGTA, 4 KCl, 10 glucose, and 10 HEPES, buffered to pH 7.4 with NaOH. Phosphate buffered saline (PBS); 137 NaCl, 2.7 KCl, 8.1 Na_2HPO_4 and 1.5 KH_2PO_4. Phosphate Buffer (0.1 M); 80 Na_2HPO_4, 20 NaH_2PO_4. Zamboni solution; 15 % saturated picric acid, 2 % paraformaldehyde in the 0.1 M Phosphate Buffer. The elastase solution was prepared by dissolving 0.1% elastase in the physiological saline. The fura-2 AM solution; 12.5 μM fura-2 AM (Molecular Probes, Eugene, OR) dissolved in Earle's solution supplemented with 1% Pluronic F-127 (Sigma). A selective mAChR subtype antagonists, 4-Diphenylacetoxy-N-methylpiperidine methiodide (4-DAMP, M3 antagonist), pirenzepine (M1 antagonist), tropicamide (M4 antagonist) and methoctramine (M2 antagonist), were obtained from Sigma.

Results

Ca^{2+} responses

A subset of TBCs substantially increased $[Ca^{2+}]_{in}$ in response to the application of ACh to their basolateral membrane side, and the repetitive application of 1 μM ACh slightly decreased the Ca^{2+} response in magnitude (Figs. 1*B* and *C*). The number of TBCs responded to 1 μM ACh per taste bud was 4.9 ± 3.1 cells (mean ± SD, n = 32). Ca^{2+} responses occurred at ACh concentrations lower than 0.01 μM, and saturated at concentrations higher than 1 μM, with the EC_{50} of 0.6 μM (n = 38, Figs. 2*A* and *B*). In the Ca^{2+}-free solution, Ca^{2+} responses to 1 μM ACh still occurred, though the response magnitude was significantly decreased ($p < 0.01$, repeated measures ANOVA and Tukey HSD multiple comparisons test, Figs.2*C* and *D*). Also, the resting level of $[Ca^{2+}]_{in}$ was decreased in the Ca^{2+}-free solution.

We pharmacologically characterized these Ca^{2+} responses in the presence of a variety of antagonists on the basolateral membrane side (Fig. 3). The addition of 100 nM atropine to 1 μM ACh significantly decreased Ca^{2+} responses to 6.7 ± 4.5 % of their respective controls in magnitude ($p < 0.001$, paired Student's *t*-test; n = 21), and the wash with the physiological saline partially reversed the inhibition. A series of subtype-selective antagonists inhibited the Ca^{2+} response with different IC_{50}s; 1.5 nM for 4-DAMP, an M3 antagonist; 0.1 μM for tropicamide, an M4 antagonist; 1.7μM for pirenzepine, an M1 antagonist; 4.0 μM for methoctramine, an M2 antagonist. The order of inhibitory potency agreed with the orders obtained from other tissues expressing M3, mouse duodenal myocytes (Morel *et al.* 1997) and guinea pig gallbladder muscles (Parkman *et al.* 1999), and suggested that M3 was responsible for Ca^{2+} responses.

Perforated whole-cell voltage-clamping

We investigated electrical responses of 13 TBCs to 1 μM ACh selectively applied to their basolateral membranes under a perforated whole-cell-clamp condition (Fig. 4). The application partially inhibited the magnitude of a voltage-gated outwardly rectifying current in one TBC, though that current remained unchanged in the other TBCs. The ACh-sensitive current developed very slowly at membrane potentials more positive than -20 mV, lasted for more than 50 ms without inactivation, and was antagonized by the addition of 100 nM atropine to the ACh solution.

PCR studies

We also investigated the expression of mAChR subtypes on fungiform TBCs with

RT-PCR, and detected a PCR product for M3 (Fig. 5). The product size agreed with the expected one, and the identity of the product was confirmed by sequencing. RT-PCR products for the other mAChR subtypes, M1, M2, M4, M5, and VAChT were undetectable. These results were consistent with the pharmacological results mentioned above.

For comparison, we investigated the expression of mAChR subtypes and VAChT in circumvallate papillae that contained taste buds and surrounding lingual epithelial cells. PCR products detected were for M1, M3, M4, M5, and VAChT, but that for M2 was undetectable (data not shown).

Immunohistostaining

In fungiform papillae, there were immunoreactive regions to an anti-VAChT antibody in horizontal, optical slices of whole-mount taste buds (Fig. 6). No immunoreactivity was detected after preadsorption of the anti-VAChT antibody with the synthetic antigen. Shifting the focal plane of confocal microscopy, we found that VAChT-immunoreactivity occurred on a few PLCβ2-immunoreactive TBCs, and that a few nerve endings, SNAP-25-immunoreactive regions having no soma-like bulges within taste buds, were also immunoreactive to both VAChT and SNAP-25. Also we investigated VAChT-immunoreactivity in circumvallate taste buds with sliced preparations (see Materials and Methods). VAChT-immunoreactivity occurred on a few IP_3R3-immunoreactive TBCs, but that on SNAP-25-immunoreactive TBCs was undetectable.

Discussion

The present results obtained with Ca^{2+} imaging, RT-PCR, and perforated whole-cell clamping cooperatively showed that fungiform TBCs expressed M3 as follows. The order of inhibitory potency yielded by Ca^{2+} imaging was 4-DAMP > tropicamide > pirenzepine > methoctramine (Fig. 3C), which agreed with the order obtained from other tissues expressing M3, mouse duodenal myocytes (Morel *et al.* 1997) and guinea pig gallbladder muscles (Parkman *et al.* 1999). Only one RT-PCR product detected in fungiform TBCs was for M3 (Fig. 5). A current obtained from a fungiform TBC assumed to be M-current as descried later supports the expression of M3 (Fig. 4), since M-current can be modulated by M3 (Marrion 1997).

The present study also suggests that TBCs or epithelial cells in circumvallate papillae express M1, M3, M4, and M5. These results agreed with previous results that immunohistochemically showed the expression of M1 in foliate and circumvallate TBCs, though the expression of mAChR subtypes other than M1 had not been examined (Ogura 2002; Ogura *et al.* 2005). It is thus likely that fungiform and circumvallate TBCs express different mAChR subtypes. The responsiveness of the chorda tympani nerve innervating fungiform TBCs is different from that of the glossopharyngeal nerve innervating circumvallate TBCs (Sako *et al.* 2000). The subtype of mAChRs on TBCs may contribute to the differences.

M3 as well as M1 and M5 is coupled to the alpha subunit of $G_{q/11}$ class G proteins results in the increase in $[Ca^{2+}]_{in}$ via the activation of PLCβ2, whereas M2 and M4 are coupled to $G_{i/o}$ class G proteins and decrease intracellular cAMP levels (Caulfield 1993; Caulfield *et al.* 1994; Felder 1995). Type II cells, partially identical to PLCβ2-immunoreactive TBCs, express G-protein-coupled taste receptors, T1Rs and T2Rs, which are coupled to the activation of PLCβ2 (Zhang *et al.* 2003). Since the alpha subunit of G_q, $G_{\alpha q}$, was expressed in rat TBCs (Kusakabe *et al.* 2000), it is likely that the present ACh-induced Ca^{2+} responses occur in Type II cells that express M3. This crosstalk between G-protein-coupled taste receptors and M3 would enhance the taste response of these Type II cells, when ACh is applied to them during taste stimulation. This hypothesis may account for previous results (Kimura 1961; Sakai 1965).

The present study detected VAChT-immunoreactivity in fungiform and circumvallate taste buds (Fig.6), suggesting that TBCs or nerve endings release ACh by exocytosis. VAChT-immunoreactive TBCs were PLCβ2-immunoreactive in fungiform taste buds,

and were IP_3R3-immunoreactive in circumvallate taste buds. Although RT-PCR failed to detect VAChT in fungiform taste buds, the failure seems to result from the fact that the number of fungiform taste buds used in the RT-PCR study was much smaller than that of circumvallate taste buds.

Both PLCβ2-immunoreactive TBCs and IP_3R3 immunoreactive TBCs are assumed to be Type II cells, which have no synaptic vesicles. Also, these VAChT-immunoreactive Type II-like cells expressed no SNAP-25. It appears that these TBCs can not release ACh by exocytosis. However, immunohistochemical classification is different from morphological classification, and not all PLCβ2-immunoreactive TBCs and IP_3R3 immunoreactive TBCs are classified into Type II (Clapp *et al.* 2004). Also, VAChT-immunoreactive Type II-like cells may express another member of SNAP family. Therefore, further studies are needed to elucidate the role of VAChT in these TBCs.

VAChT-immunoreactivity was also detected in SNAP-25-immunoreactive nerve endings in fungiform taste buds, suggesting that these nerve endings release ACh by exocytosis using SNAP-25, which generates muscarinic actions on TBCs via M3. VAChT-immunoreactive nerve endings may be postganglionic parasympathetic nerves, since they innervated TBCs in bullfrogs (Sato *et al.* 2005). Similar muscarinic actions may occur on circumvallate TBCs. Rat circumvallate and foliate TBC expressed adrenergic receptors where noradrenaline inhibited voltage-gated outward potassium currents (Herness *et al.* 2002). It is thus likely that both sympathetic and parasympathetic neurons supply TBCs and modulate their functions as found in a variety of organs.

The current obtained from a fungiform TBC was sensitive to ACh and atropine, slowly activated at membrane potentials less than -20 mV, and non-inactivated. These properties except the range of activation potentials are similar to M-current previously reported (Adams *et al.* 1982), showing that the current is M-current. Suppression of M-current usually results in membrane depolarization and an increase in input resistance, which makes the cell more likely to fire action potentials. In TBCs, its suppression would not depolarize the TBC at resting potentials because of its higher activation potentials. Although the TBC that generated M-current exhibited no voltage-gated Na^+ currents, M-current may occur on type II cells that fire action potentials. When this is the case, the suppression of M-current would elongate the width of action potentials.

In response to taste substances, TBCs generate action potentials that open hemichannels, and ATP as a neurotransmitter is released through the hemichannels (Finger *et al.* 2005; Huang *et al.* 2007; Romanov *et al.* 2007). Therefore, the suppression of M-current facilitates the ATP release, which results in the enhancement of taste nerve responses, which agree with previous studies (Kimura 1961; Sakai 1965). The channels that elicit the M-current of TBCs remain to be identified. Two voltage-gated channels, KCNQ1 and KCNH2, were found in rat TBCs in circumvallate papillae (Ohmoto *et al.* 2006). These channels may be responsible for the M-current of TBCs, since KCNQ1 and probably KCNH2 generate M-current (Jentsch 2000).

Acknowledgements

This work is partially supported by the 21st Centre of Excellence Program at the Kyushu Institute of Technology, and a Grants-in-Aid for Scientific Research (#16300094) from JSPS.

References

Adams, P.R., Brown, D.A. and Constanti, A. 1982, M-currents and other potassium currents in bullfrog sympathetic neurones, J Physiol 330: 537-572.

Caulfield, M.P. 1993, Muscarinic receptors--characterization, coupling and function, Pharmacol Ther 58: 319-379.

Caulfield, M.P., Jones, S., Vallis, Y., Buckley, N.J., Kim, G.D., Milligan, G. and Brown, D.A. 1994, Muscarinic M-current inhibition via G alpha q/11 and alpha-adrenoceptor inhibition of Ca2+ current via G alpha o in rat sympathetic neurones, J Physiol 477 (Pt 3): 415-422.

Clapp, T.R., Yang, R., Stoick, C.L., Kinnamon, S.C. and Kinnamon, J.C. 2004, Morphologic characterization of rat taste receptor cells that express components of the phospholipase C signaling pathway, J Comp Neurol 468: 311-321.

Duncan, C.J. 1964, Synaptic Transmission at Taste Buds, Nature 203: 875-876.

Felder, C.C. 1995, Muscarinic acetylcholine receptors: signal transduction through multiple effectors, Faseb J 9: 619-625.

Finger, T.E., Danilova, V., Barrows, J., Bartel, D.L., Vigers, A.J., Stone, L., Hellekant, G. and Kinnamon, S.C. 2005, ATP signaling is crucial for communication from taste buds to gustatory nerves, Science (New York, N.Y 310: 1495-1499.

Furue, H. and Yoshii, K. 1997, In situ tight-seal recordings of taste substance-elicited action currents and voltage-gated Ba currents from single taste bud cells in the peeled epithelium of mouse tongue, Brain Res 776: 133-139.

Herness, S., Zhao, F.L., Kaya, N., Lu, S.G., Shen, T. and Sun, X.D. 2002, Adrenergic signalling between rat taste receptor cells, J Physiol 543: 601-614.

Higure, Y., Katayama, Y., Takeuchi, K., Ohtubo, Y. and Yoshii, K. 2003, Lucifer Yellow slows voltage-gated Na+ current inactivation in a light-dependent manner in mice, J Physiol 550: 159-167.

Huang, Y.J., Maruyama, Y., Dvoryanchikov, G., Pereira, E., Chaudhari, N. and Roper, S.D. 2007, The role of pannexin 1 hemichannels in ATP release and cell-cell communication in mouse taste buds, Proc Natl Acad Sci U S A 104: 6436-6441.

Hwang, P.M., Verma, A., Bredt, D.S. and Snyder, S.H. 1990, Localization of phosphatidylinositol signaling components in rat taste cells: role in bitter taste transduction, Proc Natl Acad Sci U S A 87: 7395-7399.

Jentsch, T.J. 2000, Neuronal KCNQ potassium channels: physiology and role in disease, Nature reviews 1: 21-30.

Kimura, K. 1961, Factors affecting the response of taste receptors of rat., Kumamoto

Med. J. 14: 95-99.
Kusakabe, Y., Yasuoka, A., Asano-Miyoshi, M., Iwabuchi, K., Matsumoto, I., Arai, S., Emori, Y. and Abe, K. 2000, Comprehensive study on G protein alpha-subunits in taste bud cells, with special reference to the occurrence of Galphai2 as a major Galpha species, Chem Senses 25: 525-531.
Marrion, N.V. 1997, Control of M-current, Annual review of physiology 59: 483-504.
Morel, J.L., Macrez, N. and Mironneau, J. 1997, Specific Gq protein involvement in muscarinic M3 receptor-induced phosphatidylinositol hydrolysis and Ca2+ release in mouse duodenal myocytes, Br J Pharmacol 121: 451-458.
Ogura, T. 2002, Acetylcholine increases intracellular Ca2+ in taste cells via activation of muscarinic receptors, J Neurophysiol 87: 2643-2649.
Ogura, T. and Lin, W. 2005, Acetylcholine and acetylcholine receptors in taste receptor cells, Chem Senses 30 Suppl 1: i41.
Ohmoto, M., Matsumoto, I., Misaka, T. and Abe, K. 2006, Taste receptor cells express voltage-dependent potassium channels in a cell age-specific manner, Chem Senses 31: 739-746.
Ohtubo, Y., Suemitsu, T., Shiobara, S., Matsumoto, T., Kumazawa, T. and Yoshii, K.Y. 2001, Optical recordings of taste responses from fungiform papillae of mouse in situ, J Physiol 530: 287-293.
Paran, N. and Mattern, C.F. 1975, The distribution of acetylcholinesterase in buds of the rat vallate papilla as determined by electron microscope histochemistry, J Comp Neurol 159: 29-44.
Parkman, H.P., Pagano, A.P. and Ryan, J.P. 1999, Subtypes of muscarinic receptors regulating gallbladder cholinergic contractions, The American journal of physiology 276: G1243-1250.
Romanov, R.A., Rogachevskaja, O.A., Bystrova, M.F., Jiang, P., Margolskee, R.F. and Kolesnikov, S.S. 2007, Afferent neurotransmission mediated by hemichannels in mammalian taste cells, The EMBO journal 26: 657-667.
Sakai, K. 1965, Studies on Chemical Transmission in Taste Fibre Endings. II. The Effect of Cholinesterase Inhibitor on the Taste, Chem Pharm Bull (Tokyo) 13: 304-307.
Sako, N., Harada, S. and Yamamoto, T. 2000, Gustatory information of umami substances in three major taste nerves, Physiology & behavior 71: 193-198.
Sato, T., Okada, Y., Miyazaki, T., Kato, Y. and Toda, K. 2005, Taste cell responses in the frog are modulated by parasympathetic efferent nerve fibers, Chem Senses 30: 761-769.
Zhang, Y., Hoon, M.A., Chandrashekar, J., Mueller, K.L., Cook, B., Wu, D., Zuker,

C.S. and Ryba, N.J. 2003, Coding of sweet, bitter, and umami tastes: different receptor cells sharing similar signaling pathways, Cell 112: 293-301.
Zimring, J.C., Kapp, L.M., Yamada, M., Wess, J. and Kapp, J.A. 2005, Regulation of CD8+ cytolytic T lymphocyte differentiation by a cholinergic pathway, Journal of neuroimmunology 164: 66-75.

Tables

TABLE 1. Primers used in this study.

Gene Target		Sequence	Product Size (bp)	Ref.
mAChR M1	Forward	5'-GTAAGGTGCCTGCCATCCAATC-3'	417	NM_007698
	Reverse	5'-CGCAGCTCACTTTCTGCATTGT-3'		
mAChR M2	Forward	5'-TGTCAGCAATGCCTCCGTTATG-3'	480	(Zimring *et al.* 2005)
	Reverse	5'-GCCTTGCCATTCTGGATCTTG-3'		
mAChR M3	Forward	5'-GGTGTGATGATTGGTCTGGCTTG-3'	497	(Zimring *et al.* 2005)
	Reverse	5'-GAAGCAGAGTTTTCCAGGGAG-3'		
mAChR M4	Forward	5'-TCAAGAGCCCTCTGATGAAGCC-3'	477	(Zimring *et al.* 2005)
	Reverse	5'-AGATTGTCCGAGTCACTTTGCG-3'		
mAChR M5	Forward	5'-GCTGACCTCCAAGGTTCCGATTC-3'	485	(Zimring *et al.* 2005)
	Reverse	5'-CCGTCAGCTTTTACCACCAAT-3'		
VAChT	Forward	5'-GCCACGTGGATGAAGCACAC-3'	487	NM_021712
	Reverse	5'- GAGGCCCACATTACGCAAG-3'		
α-gustducin	Forward	5'-CTCTTCCAGGAGAAAGTGGC-3'	248	XM_144196
	Reverse	5'- TCAGAAGAGCCCACAGTCTT-3'		
β-actin	Forward	5'-GTAAAGACCTCTATGCCAACAC-3'	289	NM_007393
	Reverse	5'-GTGTAAAACGCAGCTCAGTAAC-3'		

TABLE 2. Antibodies used for immunofluorescence labeling

Antiserum	Type of antibody	Coupled to	Dilution	Origin
Primary				
VAChT (human)	Goat polyclonal	-	1:500	1
PLCβ2 (human)	Rabbit polyclonal	-	1:100	2
IP_3R3 (human)	Mouse monoclonal		1:50	3
SNAP-25 (human)	Mouse monoclonal	-	1:1000	4
Secondary				
Rabbit IgG	Donkey	Alexa Fluor 488	1:400	5
Mouse IgG	Donkey	Alexa Fluor 555	1:400	5
Goat IgG	Donkey	Alexa Fluor 633	1:200	5

1 = CHEMICON International, Temecula, CA; 2 = Santa Cruz Biotechnology, Santa Cruz, CA; 3 = BD Biosciences, San Diego, CA; 4 = Sigma-Aldrich, Saint Louis, MO; 5 = Molecular Probes, Eugene, OR.

Figure legends

Fig.1. Ca^{2+}-imaging scheme (A) and Ca^{2+} responses of single fungiform TBCs to 1 μM ACh repetitively applied to the basolateral membrane side of TBCs (B and C). Normalized responses, the peak height of each Ca^{2+} response divided by that of the first Ca^{2+} responses obtained from their respective TBCs, were plotted as a function of time after the onset of the repetitive stimulation. n = 14.

Fig.2. Ca^{2+} responses recorded under different conditions. *A*, Ca^{2+} responses of a fungiform TBC to a concentration series of ACh. *B*, concentration-response relationship for ACh. Ca^{2+} responses were calculated relative to the magnitude of the response to 10 μM ACh in each TBC. EC_{50}, 0.55 ± 0.71 μM (n = 38). *C*, typical Ca^{2+} responses to 1 μM ACh in a Ca^{2+}-free solution. The basolateral membrane side was acclimated to the Ca^{2+}-free solution, irrigated with 10 μM ACh dissolved in the Ca^{2+}-free solution, and washed with the Ca^{2+}-free solution. *D*, Ca^{2+} responses to 10 μM ACh in the Ca^{2+}-free solution. The magnitude of Ca^{2+} responses examined in the Ca^{2+}-free solution and that in the physiological saline after the wash was calculated relative to the magnitude of Ca^{2+} responses recorded in the physiological saline before the irrigation with the Ca^{2+}-free solution. The magnitude of Ca^{2+} responses was significantly smaller in the Ca^{2+}-free solution than in the physiological saline (*$P < 0.01$, repeated measures ANOVA and Tukey HSD multiple comparisons test, n = 16).

Fig.3. Inhibition of Ca^{2+} responses by muscarinic antagonists. *A*, typical responses of a single TBC to 1μM ACh in the presence of 0.1 μM atropine. *B*, inhibition curves of subtype-specific antagonists for Ca^{2+} responses to 1μM ACh. Symbols; closed circles, 4-DAMP; open circles, tropicamide; closed squares, pirenzepine; open squares, methoctramine. The magnitude of Ca^{2+} responses was calculated as relative to that in the absence of antagonists in each TBC. Each point of data is obtained from 3~15 TBCs.

Fig.4. Voltage-gated outwardly rectifying currents of a fungiform TBC inhibited by ACh. *A*, a family of voltage-clamp currents. The voltage steps range from -50 to 50 mV in 10-mV increments from a holding potential of -70 mV. *B*, current-voltage relations recorded before (closed circles), during the application of 1 μM ACh (open circles), during the application of 1 μM ACh in the presence of 100 nM atropine, (open squares), and after wash with the physiological saline (closed squares). *C*, ACh-sensitive

currents elicited by a test potential to 50 mV from a holding potential of -70 mV. The ACh-sensitive currents are obtained by subtracting record without 1 μM ACh from record with it. *D*, current-voltage relation for ACh-sensitive currents obtained by the subtraction, as in *C*.

Fig.5. PCR-amplified products from cDNA reverse-transcribed from mRNA isolated from fungiform TBCs. Oligonucleotide primers specific for five different mAChR subtypes are run in separate reactions and the products run on agarose gel electrophoresis. The sequences of primers and expected product size of each reaction is listed in Table 1. Oligonucleotide primers specific for β-actin and α-gustducin are similarly examined as positive controls. H_2O used in RT-PCR experiments is also examined as a negative control. Identical aliquots of a single mRNA for each tissue were used as templates for the RT-PCR reactions shown. Identical results were obtained with three additional preparations of RNA from taste buds.

Fig.6. Immunohistochemical images of VAChT in fungiform taste buds (*A*-*C*) and in circumvallate taste buds (*D*). *A*, immunofluorescence of VAChT (green) and their overlay on a Normarski image of the same section. *B*, no selective labeling was observed in control section, in which the primary antibody was preadsorbed with the synthetic antigen. *C*, immunofluorescence of VAChT (green), PLCβ2 (red), SNAP-25 (blue), and their overlay on a Nomarski image of the same section. Immunoreactivity for VAChT occurs on PLCβ2-immunoreactive TBCs, SNAP-25-immunoreactive nerve endings (arrows). *D*, immunofluorescence of VAChT (green), IP_3R3 (red) and their overlay, and the overlay on a Normarski image of the same section. VAChT-immunoreactivity occurs on IP_3R3-immunoreactive TBCs. *E*, immunofluorescence of VAChT (green), SNAP-25 (red), their overlay, and the enlargement of the overlay. No VAChT-immunoreactivity occurs on SNAP-25-immunoreactive TBCs. Scale bar = 10 μM.

Fig.1

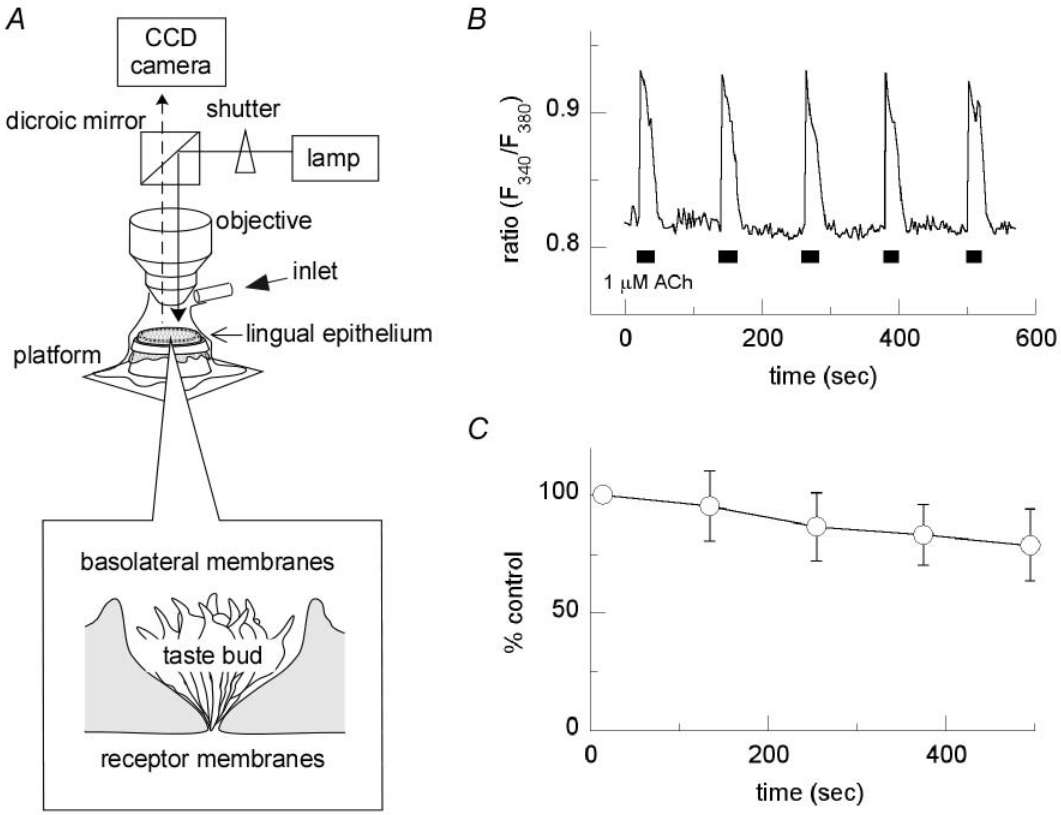
A
CCD camera
dicroic mirror
shutter
lamp
objective
inlet
lingual epithelium
platform
basolateral membranes
taste bud
receptor membranes
B
ratio (F340/F380)
0.9
0.8
1 μM ACh
0
200
400
600
time (sec)
C
% control
100
50
0
0
200
400
time (sec)

Fig.2

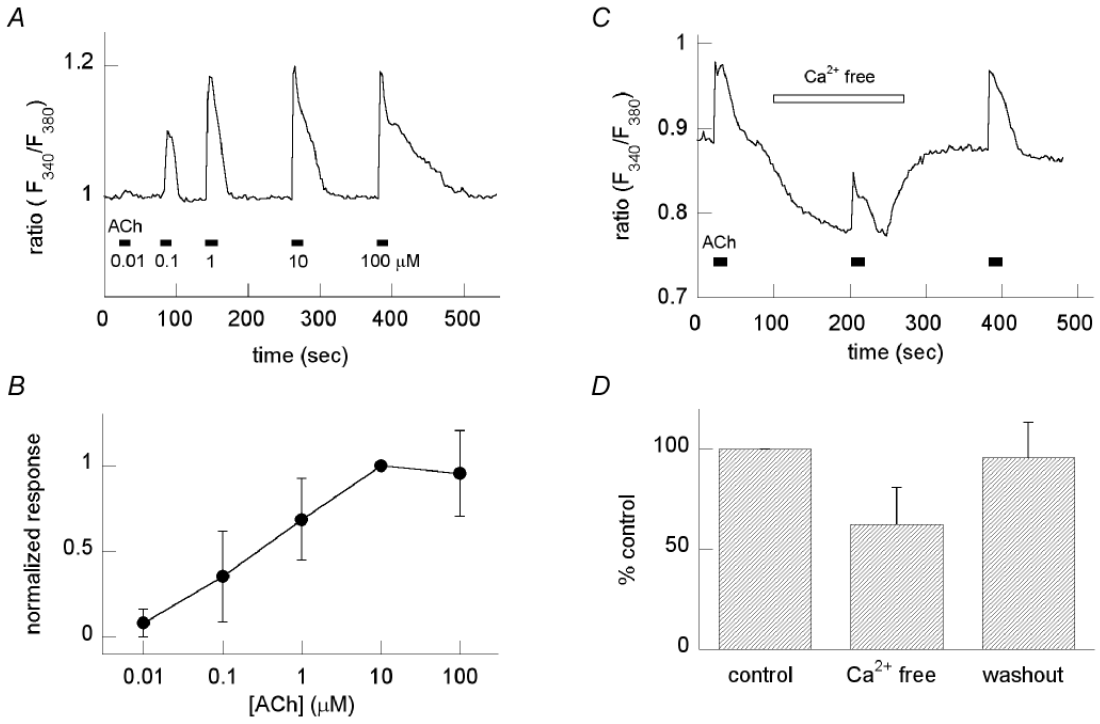
A
ratio (F340/F380)
1.2
1
ACh
0.01 0.1 1 10 100 μM
0 100 200 300 400 500
time (sec)
C
ratio (F340/F380)
1
0.9
0.8
0.7
Ca2+ free
ACh
0 100 200 300 400 500
time (sec)
B
normalized response
1
0.5
0
0.01 0.1 1 10 100
[ACh] (μM)
D
% control
100
50
0
control
Ca2+ free
washout

Fig.3

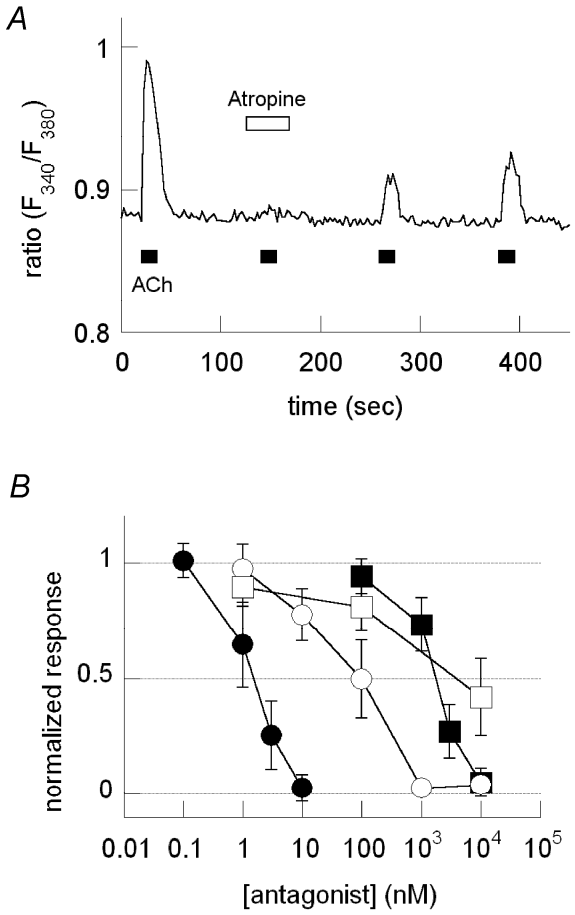
A
1
0.9
0.8
ratio (F_{340}/F_{380})
Atropine
ACh
0
100
200
300
400
time (sec)
B
1
0.5
0
normalized response
0.01
0.1
1
10
100
10^3
10^4
10^5
[antagonist] (nM)

Fig.4

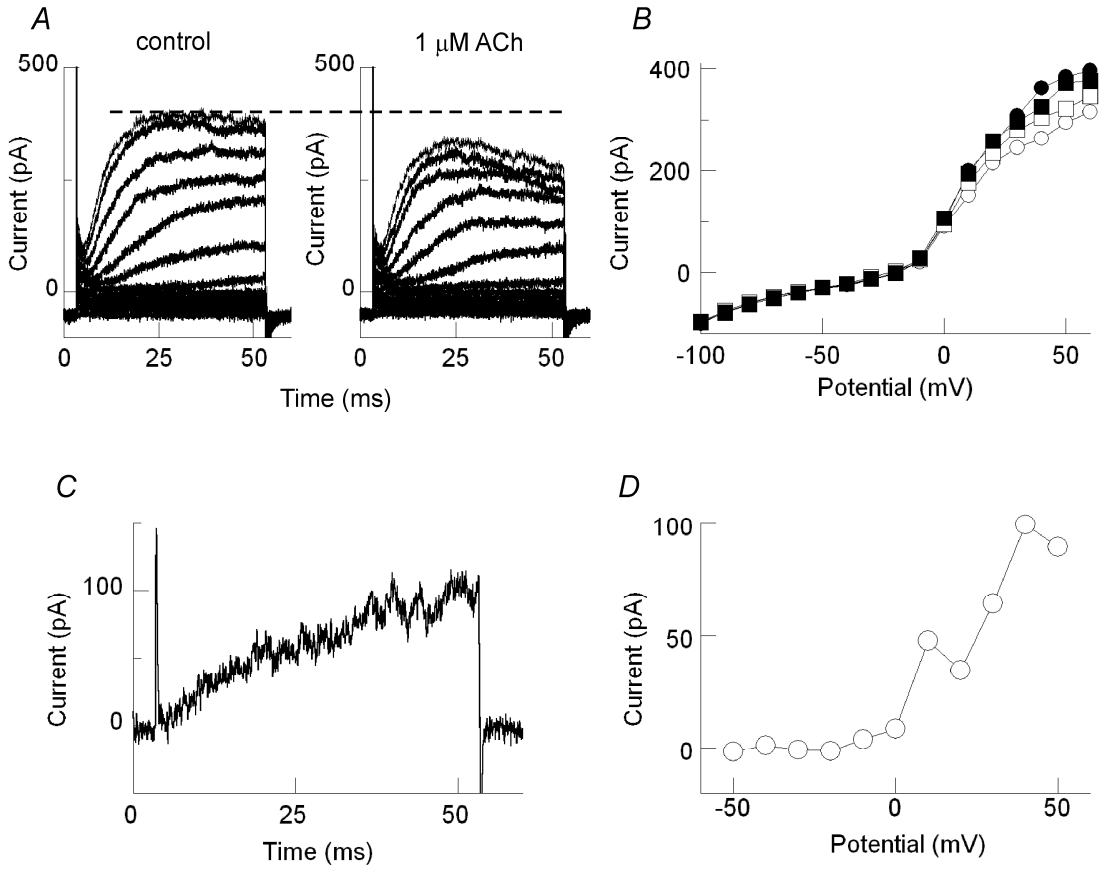
A
control
1 μM ACh
500
0
Current (pA)
0
25
50
Time (ms)
B
400
200
0
-100
-50
0
50
Potential (mV)
C
100
0
Current (pA)
0
25
50
Time (ms)
D
100
50
0
Current (pA)
-50
0
50
Potential (mV)

Fig.5

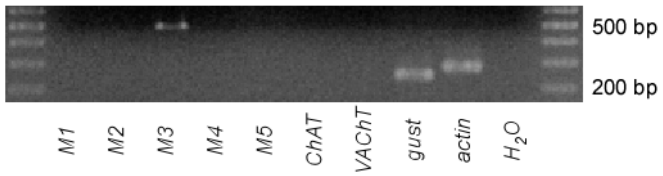

Fig.6

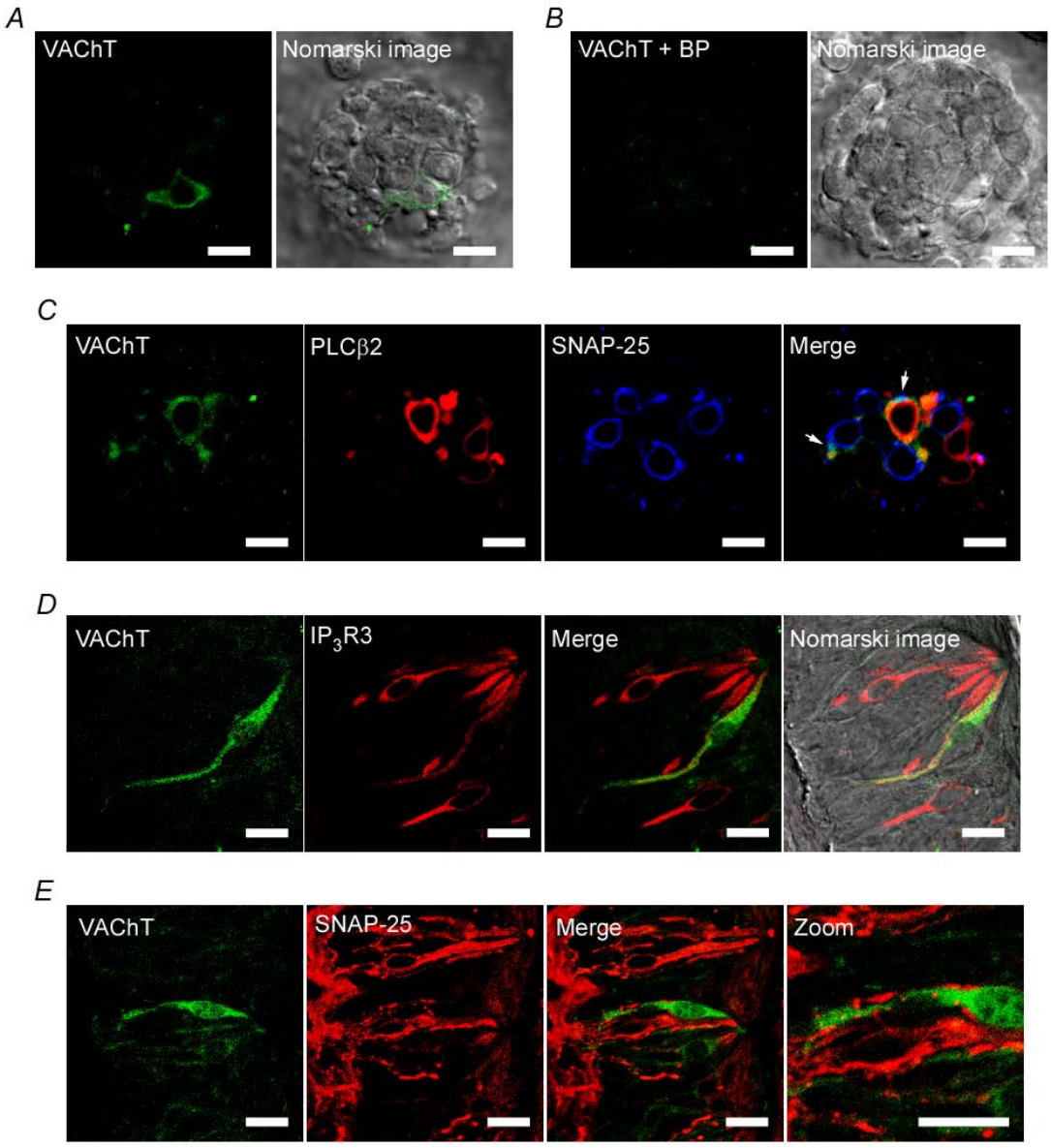
A
VAChT
Nomarski image
B
VAChT + BP
Nomarski image
C
VAChT
PLCβ2
SNAP-25
Merge
D
VAChT
IP3R3
Merge
Nomarski image
E
VAChT
SNAP-25
Merge
Zoom